PARAMAGNETIC IMPURITIES AND DEFECTS IN SILICON CARBIDE POLYTYPES

NITROGEN

Nitrogen is the common donor in all SiC polytypes and dominates the electrical properties of n-type SiC which is used as substrates for the fabrication of high-power electronic devices.

Nitrogen donors were investigated with EPR at 140 GHz and with ENDOR at 9 GHz in 6H, 4H and 15R-SiC. The number of nitrogen EPR spectra turned out to be equal of inequivalent positions of nitrogen in the SiC polytypes. The hexagonal site donors in SiC polytypes show more than 10 times smaller isotropic and also anisotropic hyperfine (HF) interactions compared to the donors on quasicubic sites which show only isotropic HF interactions. As a result the ground state of the nitrogen in quasicubic sites is described by fully symmetric $1S(A_1)$ states while anisotropic HF interactions for hexagonal site donors are explained by admixture of the 1S(E) excited state to the $1S(A_1)$ ground state due to the small value of the valley-orbit splitting for hexagonal sites. This conclusion is supported by the investigation of the temperature behavior of the HF splitting for nitrogen substituting quasicubic and hexagonal site. A reduction of the HF interaction with increasing temperature is explained by thermally activated transition of donor electrons from the $1S(A_1)$ state to the 1S(E) state which has a node at the central N atom. Optical recharging of nitrogen between two paramagnetic $1S(A_1)$ and 1S(E) states was discovered after cooling the 6H SiC samples under interband illumination.

The investigation of the ligand HF structure in EPR and ENDOR spectrum due to interaction of the unpaired electron spin with Si^{29} and C^{13} nuclear spin makes it possible to identify the type of the site substituting by nitrogen in SiC. It was concluded that nitrogen substitutes carbon site in 6HSiC and 4H SiC. The temperature dependences of donor EPR line intensities were found to deviate from the Curie law. The temperature dependencies of the line intensities and widths were used to determine ionization energies and the valley-orbit splitting of nitrogen on the quasi-cubic and hexagonal sites. The low temperature hopping motion of the donor electron between paramagnetic and nonparamagnetic state has been established and investigated in 6H and 4H-SiC heavily doped with nitrogen.

It is well known that only a part of the chemically incorporated nitrogen is electrically active, which may be explained by an increased probability that nitrogen forms complex which could be responsible for the reduction of the free carrier concentration in n-type SiC highly doped with N.

Last activities of the lab is devoted to the EPR, ESE and pulse ENDOR study of the nitrogen-related centers participating in nitrogen deactivation process in n-type 4H-SiC wafers grown by different technologies.

BORON

The shallow boron acceptors in 6H, 4H and 3C SiC were investigated with EPR at 140 GHz in the temperature interval 4.2–100 K. The microscopic model suggested from the EPR and ENDOR data including principle values of g-tensors, HF interaction constants and frequency dependent thermally activated transition of boron EPR spectra in quasi-cubic site from monocline symmetry to axial is as follows: shallow boron viewed as B-induced C acceptors. The hole is located in the connection line between B_{Si} and adjacent C, which is relaxed towards the B^{-}_{Si}.

SEMI-INSULATING (SI) SIC

The EPR and photo EPR studies have shown that SI 4H and 6H SiC reveal a series of photosensitive paramagnetic centers including boron, nitrogen and thermal highly stable deep intrinsic defects labeled X and P in 4H and XX and PP in 6H SiC. It was established that SI properties of 4H, 6H SiC were controlled by two deep intrinsic defects X, P and XX, PP, residing quasi-cubic (c) and hexagonal sites (h) with closely located energy levels in the band gap. In the dark the Fermi level is pinned at the X defect in 4H and XX defect in 6H SiC, while P and PP defect appeared under photo excitation.

1.2.1. EPR results.

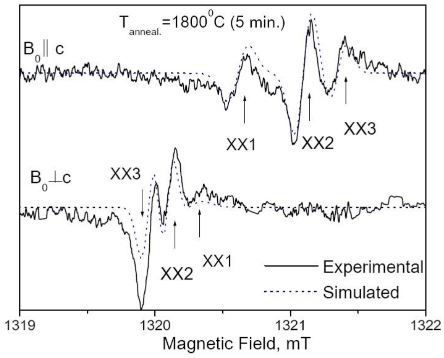

Fig.1. EPR spectrum of the XX defect measured in SI 6H SiC in the dark at 77 K and 37 GHz.

At 77 K a series of undoped SI 4H, 6H SiC samples annealed at 1800°C revealed two and three EPR lines labeled X1, X2 in 4H SiC and XX1, XX2, XX3 in 6H SiC with axially symmetric g-factors corresponding to the two and three inequivalent lattice positions of defects with S=1/2 in 4H, 6H SiC, respectively. Fig. 1 shows the Q-band EPR spectrum of the XX defect in an annealed SI 6H-SiC sample recorded at 77 K. Thus, the position of the Fermi level in the dark in undoped SI 4H and 6H SiC are determined by the energy level of X and XX center, respectively. Below 50 K the symmetry of the X and XX EPR spectra residing on quasi-cubic sites were reduced from axial C_{3v} to a lower symmetry, while the axial symmetry of the EPR spectrum due to the X and XX defect residing on the hexagonal site remains. The EPR parameters of the X and XX defects obtained from fitting the experimental spectrum with simulated one are given in Table 1. For comparison the parameters of so-called Ky1, Ky2, Ky3 EPR spectra observed in p-type electron irradiated 6H SiC, which have been associated to the V_C^+, are given in Table 1. Quite similar g-tensors and symmetry features of XX and the Ky EPR spectra enable us to tentatively attribute the XX EPR to the V_C^+.

Table 1. Energy levels and EPR parameters of 6H-SiC XX, and 4H-SiC X defects with S= 1/2 and the parameters of the Ky1, Ky2, Ky3 centers observed in p-type electron irradiated 6H SiC at 77 K.

	XX3(h)	**XX2(c)**	**XX1(c)**	**Ky3(h)**	**Ky2**	**Ky1**	**X1(h)**	**X2(c)**
$g_{\|\|}$	2.0024	2.0027	2.0035	2.0025	2.0028	2.0036	2.0025	2.0028
$g_\perp$	2.0045	2.0043	2.0040	2.0045	2.0043	2.0041	2.0044	2.0043
$(E_V + E_i)$, [eV]	1.24						1.9	2.00
Polytype	6H						4H	

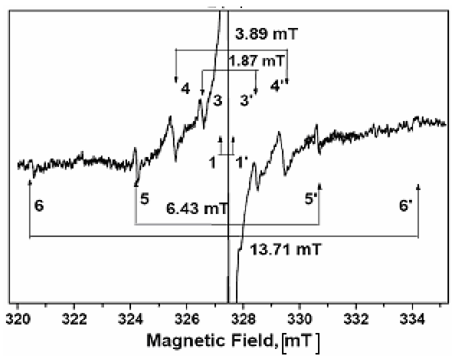

Fig. 2. EPR spectrum of the X-defect along with ligand hf structure due to ^{29}Si measured in SI 4H SiC in the dark at 77K and 9.18 GHz. **B_0||c**.

The identification of the X defect in 4H SiC was performed on the base of analysis of the ligand hyperfine splitting (hfs) observed in the X-band EPR spectrum of the defect: X1(h) and X2(c) EPR signals are superimposed and the EPR spectrum consists of a single line with a slightly asymmetric line shape at **B_0||c** (Fig. 2). Besides the strong central line, six weaker satellite lines (labeled 1 to 6) are found symmetrically around the central line. A comprehensive analysis of the complete angular dependence of all satellites ends up with a fingerprint as given in for the Si- nearest neighbors (NN) of the carbon vacancy, both at the cubic (ID1/EI5-center) and hexagonal (ID2/EI6-center) lattice sites (Table 1). However, a surprising fact was o discovered: for the inner hfs of 0.39mT (1-1') the intensity ratio between central line and satellite is different for X1(c), ID1 and E15 centers. For the X1 defect the intensity ratio is by one order of magnitude too high if compared with that observed for ID1/EI5-center. Since the hfs is the same in all cases, but the number of nuclei involved is different, one has to suggest a common additional rather small disturbance of C_V. The twofold hfs suggests that a nucleus with nuclear spin I=1/2 and high (probably 100%) natural abundance is involved. The most probable candidate is hydrogen (H), which e.g. also in Si provokes a small disturbance of defects, introduced by sample preparation and only hardly observable with EPR. According to our analysis, in the present sample about 20% of V_C would be contaminated with H.

1.2.2. Photo EPR results

The study of the photo excitation and quenching of the EPR spectrum in SI 4H and 6H SiC shows that a number of impurities and defects such as nitrogen (N), boron (B), P, PP defects are in a non-EPR active state in the dark. Excitation of the samples with light gives rise to photo quenching of the X and XX defects and transition of N, B and P, PP, defects from a diamagnetic ground state into observable paramagnetic states depending on the location of the quasi Fermi level at a given temperature. The parameters of the P and PP defects observed in SI 4H and 6H SiC samples under photo excitation are given in Table 2. The energy level of the X, XX and P, PP defects were obtained from the study of spectral dependencies of EPR spectra (Table 1, 2).

Table 2. Energy levels and parameters of the PP and P EPR spectra with S= 1/2 and C_{3V} symmetry observed in SI 6H SiC and SI 4H SiC at 77 K.

	PP (h)	**P1 (h)**	**P2 (c)**
$g_{\|\|}$	2.0047	2.0048	2.0037
$g_{\perp}$	2.0028	2.0030	2.0037
(E_V+E_i), [eV]	1.29	2.1	
Polytype	6H	4H	

As was seen from Table 1 and 2, the photo-EPR measurements result in donor-like energy levels for the X and P defects in SI 4H SiC while those in SI 6H SiC result in acceptor-like energy levels for the XX, PP defects. Based on the C_{3V} symmetry of the P EPR spectrum, energy levels and the ligand hf interactions with carbon in the NN shell, the P center is identified as an isolated silicon vacancy V_{Si}^{3-}. Currently theoretical calculations are on the way, also taking into account possible vacancy clusters. Considering that the parameters of PP defect fit well with those of P defect, the PP defect could be attributed to the same type of defect possibly in another charge state with an energy level in the low half of the band gap.

1.2.3. Theoretical calculations and electronic model of X defect.

The donor-like energy level of the X defect and the fact that the Fermi level in SI 4H SiC is pinned in the upper half of the band gap at an energy close to that of the X defect supports the conclusion that the X defect is related to hydrogenated carbon vacancies (V_C+H). The theoretical calculations show that V_C with adjacent hydrogen (V_C+H) has a significant higher ionization energy than that for $V_C^{+/0}$ (see Table 2). Fig. 3 shows the ground state configuration of a neutral (V_C+H) pair giving rise to a S=1/2 singlet. In accordance with theoretical calculations performed in the framework of density functional theory, hydrogen is built in bond-bridging between two Si-ligands of V_C. The hfs has been calculated for various configurations of the (V_C+H). The H-atom in the center of three ligands Si_3, Si_4 and Si_2 provides nearly isotropic hf parameters which are in reasonable agreement with experimental values of ligand hfs for 1-1' satellites.

Table 2. Ionization levels [eV] in respect to the valence band of the isolated V_C and (V_C+H) from experiment and theory.

Experim.	Theory	Model
1.47	1.57	$V_C^{+/0}$ acceptor
1.90, 2.00	2.05	$(V_C\text{+H})^{0/-}$ donor

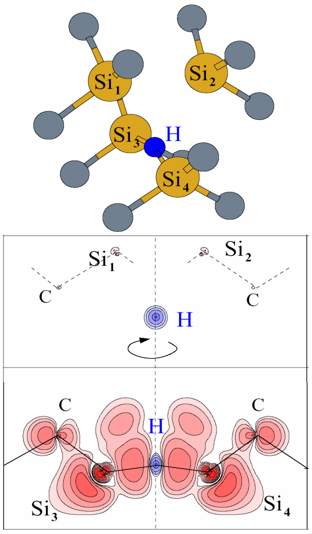

Fig. 3. Calculated ground state geometry and corresponding spin-density (in two perpendicular planes) of the (V_C+H) at the quasi-cubic site in 4H-SiC.

1.2.5. Persistent photoconductivity (PPC) effect in SI 4HSiC.

The principle feature of SI SiC is that the lifetime of the electrons and holes captured at the defect and impurity levels is very long, about 14-20 hours and more at low temperature, and is accompanied by PPC effect. The decay kinetics of the PPC was found to follow a stretched exponential form. The PPC in ΔT=77-300K was found to be produced by a thermally induced charge transfer process involving deep trap levels identified as X and P.

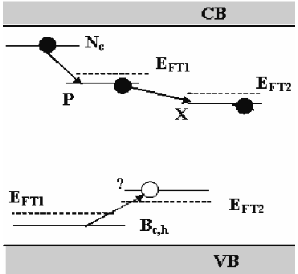

Fig. 4: Temperature induced charge transfer process in SI 4H SiC.

6. Electronic model of trapping recombination process occurred in SI 4H and 6H SiC.

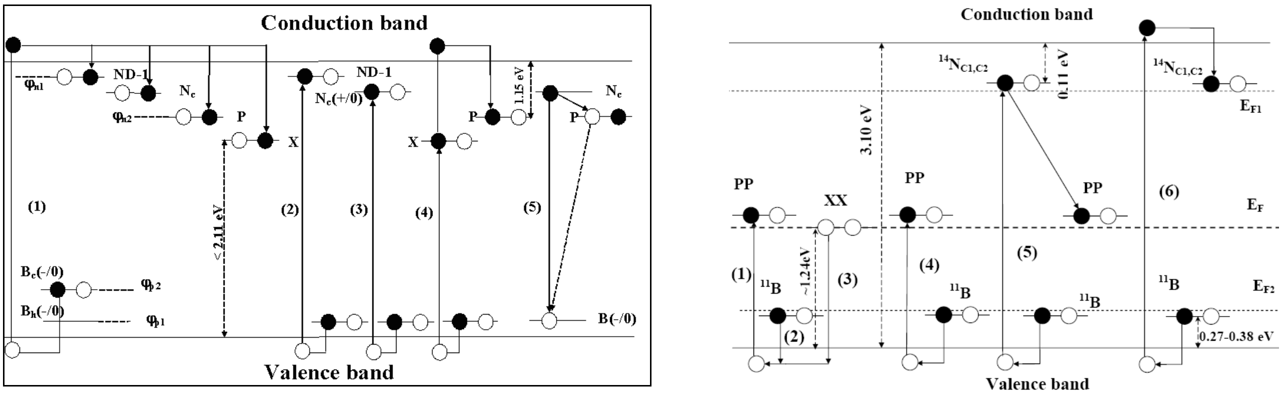

Fig. 5. Electronic scheme describing the behavior of the photosensitive paramagnetic centers observed in n-type SI 4H (1) and p-type SI 6H (2) SiC under photo excitation.

Thus, the analysis of the physical properties of intrinsic defects incorporated into SI SiC and technology preparation of the SI material gave rise to conclusions which may have impact on the development on the general principles of growing SI material of n- or p-type behavior.

It was established that SI properties of 4H and 6H SiC are controlled by two thermal highly stable deep intrinsic defects due to carbon and silicon related vacancy complexes, which have closely located energy levels. Depending on the hydrogen contamination of the wafer the energy levels of the defects responsible for the SI SiC properties are located in the upper half or lower half of the band gap and carbon vacancies would be contaminated with hydrogen forming a (V_C+H) pair. This conclusion may have a great impact on the technology progress of SI material with controlled yield and will stimulate further *ab-initio* calculations directed to structural optimization of the (V_C+H) pair configurations.